Dynamic group velocity control in a mechanically tunable photonic-crystal coupled-resonator optical waveguide

Kehan Tian,[1,][*] William Arora,[2] Satoshi Takahashi,[2] John Hong,[3] and George Barbastathis[4]

[1]*IBM Semiconductor Research and Development Center, Hopewell Junction, New York 12533, USA*

[2]*Department of Mechanical Engineering, Massachusetts Institute of Technology, 77 Massachusetts Avenue, Cambridge, Massachusetts 02139, USA*

[3]*Qualcomm, 5775 Morehouse Drive, San Diego, California 92121, USA*

[4]*Singapore-MIT Alliance for Research and Technology (SMART) Center, Block S16-06-17, 3 Science Drive 2, Singapore 117543, Singapore*

We describe a tunable slow light device based on a photonic-crystal with a mechanically adjustable coupled-resonator optical waveguide structure. The lateral energy confinement is implemented along a lattice shear defect with the group velocity actively controlled by shifting the shear along the defect interface over a distance of one crystal period. The group velocity tuning range can be anywhere from arbitrarily small (determined by the waveguide structure) to near the value expected in bulk media. We present the theory and a demonstration (via simulation) of a device configuration that is realistic to fabricate and achieves a tunable range of group velocity spanning at least three orders of magnitude. The conditions for stopping the light are also discussed for different configurations.

I. INTRODUCTION

Active control of the propagation characteristics of a light wave signal, e.g., speed, is important to the development of fast access optical memories and optically controlled delay lines in optical communication systems and optical computing. We present a method of controlling the group velocity within a photonic-crystal waveguide by mechanically moving part of the waveguide by submicrometer distances. Our proposed approach is unique in that it only engineers structure configuration to control the group velocity. It does not require special media such as cold atomic gases,[1,2] electronic transitions in crystalline solids,[3] or other nonlinear optical[4,5] and thermal[6] effects. Thus, our approach is applicable at any wavelength range, particularly in the low loss window of optical devices and highly flexible because it is decoupled from nonlinear, thermal, and other effects that may be used in optical systems for other purposes.

Our concept is to laterally translate one-half of a photonic-crystal with respect to the other half. We have previously shown that a shear-type defect within a two-dimensional (2D) photonic-crystal [Figs. 1(a) and 1(b)] supports guided modes, and furthermore, that the shear amount controls a number of mode properties including group velocity and dispersion.[7] For pedagogical purposes, we review this operational principle in Sec. II using a simplified structure which is impractical for standard fabrication techniques. In Sec. III of this paper, we introduce a design that is feasible from a fabrication perspective and also tolerant to the implementation errors that are likely to arise from fabrication and operation.

Still, one of the main operational limitations of this structure is the large group velocity dispersion. In Sec. IV we introduce a photonic structure, a shearable coupled-resonator optical waveguide (CROW). This is a CROW made within a photonic-crystal lattice by removing selected dielectric struc-

tures to form resonant cavities that are evanescently coupled. If the waveguide is made along a straight line, it is possible to shear it as shown in Figs. 1(c) and 1(d). This effectively changes the coupling coefficients between resonant cavities and allows control over the group velocity of light. The properties of eigenstates of sheared CROWs, such as symmetry and field distribution, are also investigated. Using finite-difference time-domain (FDTD) simulations, we demonstrate the process of tuning group velocity by changing the shear shift only. Mechanical displacements of only half a lattice constant are required (submicrometer for optical applications), and the device can operate at any frequency range.

The sheared CROW is limited by the minimum group velocity achievable with zero shear. Spacing the CROW cavities farther apart lowers the minimum group velocity, but may be practically limited by the size of waveguide required. In Sec. V we attempt to extend the tuning range until we create a flat band state (zero group velocity) by using the resonant side cavity concept.[8,9] We are able to show that the group velocity can be tuned over a range of three orders of magnitude. We also derive the possibility and conditions to achieve flat band state for different structures. Therefore, light entering this structure can be reversibly slowed by adiabatically modulating the amount of shear.

II. LOCALIZED PROPAGATION MODES IN PHOTONIC-CRYSTALS HAVING SHEAR DISCONTINUITIES (Ref. 7)

Consider a conventional 2D photonic-crystal consisting of dielectric rods in air on a square array with lattice constant a as shown in Fig. 1(a). For definiteness, we assume that the refractive index of the rods is 3.0 and the radius is $r=0.2a$. The crystal has a TM (magnetic field in plane) band gap which extends from frequency $\omega=0.323\times2\pi c/a$ to $\omega=0.443\times2\pi c/a$. This range corresponds to the canonical
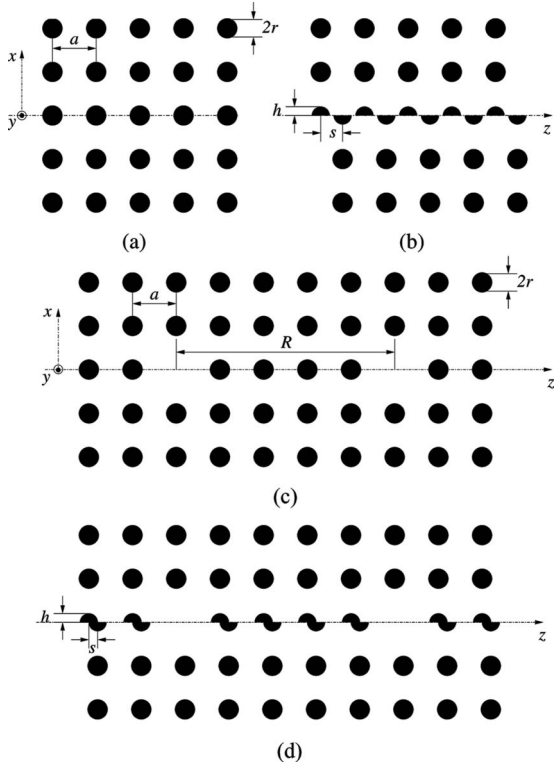
FIG. 1. Overhead view of 2D photonic-crystals comprising dielectric rods on a square lattice in air. (a) A perfect 2D crystal with lattice constant a and rod radius $r=0.2a$. (b) The same crystal, sheared through a row of cylinders at position h with one half of the crystal laterally translated by a distance s, in this case $h=r$ and $s=a/2$. (c) The same 2D crystal as in (a) but with periodic CROW defects (missing rods every $5a$). (d) The CROW with a shear discontinuity. As in (b), half of the crystal is laterally translated by a distance s.

free-space wavelength of light between 451 and 619 nm when $a=0.2$ μm. In this paper, we restrict our analysis to TM modes.

We presented a discontinuity in the middle row as shown in Fig. 1(b).[7] The circular dielectric rods in the middle line are cut in half so that the height $h=r$ and the shear shift s ranges from 0 to $0.5a$. The band diagram is computed by solving Maxwell equations directly in Fourier domain[10] and illustrated in Fig. 2. As the shear is increased, the bands above and below the band gap pull together, creating guided modes bound to the interface within the bulk of the crystal. Near the edge of the Brillouin zone, X ($k=\pi/a$), the modes flatten out and the group velocity is nearly zero (over a very small bandwidth). When $s=0.5a$, no flattening happens at the edge of Brillouin zone. This property is unlike the conventional photonic-crystal waveguides.

The guided modes in the shear waveguide have very low group velocity dispersion. Intuitively, this is because the local period along the shear plane has decreased to $a/2$ instead of a, breaking the condition for strong backward distributed Bragg reflection (DBR) coupling.[29] It is DBR that causes the flattening of dispersion curves of conventional photonic-crystal waveguides.[7,11] Moreover, the absence of dispersion flattening curve eliminates the mode gap:[12] guided modes cover the full band gap.
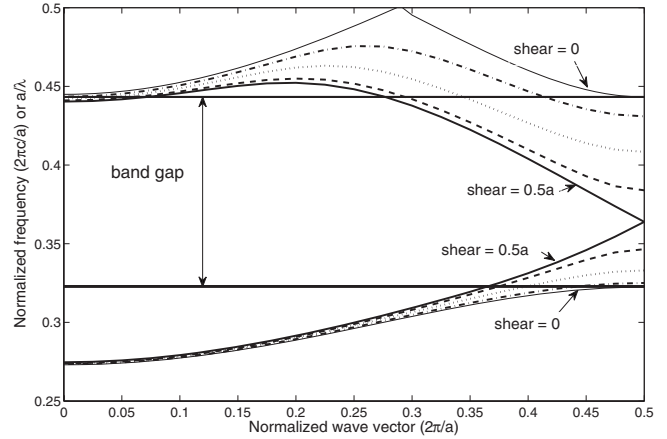

FIG. 2. The two optical modes above and below the band gap of the crystal for increasing shear amounts, plotted along the X direction in reciprocal space. When $s=0a$, the structure is a perfect photonic-crystal and the modes form the expected band gap. As the amount of shear increases, the modes move within the band gap, and at $s=0.5a$, all frequencies within the band gap can propagate along the shear while being confined by the bulk crystal. For an optical input centered around a particular frequency, for example, $0.42 \times 2\pi c/a$, as s is tuned from 0.5 to about 0.2 the group velocity decreases from about $0.4c$ to nearly zero and then for $s<0.2$ the mode cannot propagate.

III. ALTERNATE DESIGN FOR PRACTICAL IMPLEMENTATION

Fabricating a 2D photonic-crystal and shearing it as shown in Fig. 1(b) would be exceedingly difficult using a surface micromachining process. This is because of the requirement of making the cut on a free-standing structure that is capable of sliding laterally in a small region of a larger optical waveguide. In addition, the earlier design is poor because it suffers from a number of problems that will reduce optical coupling and confinement such as vertical motion at the shear interface. An alternate approach is to fabricate a similar structure by folding or stacking a patterned membrane, using one of the approaches we have previously demonstrated such as ion-implantation stress[13] or magnetically actuated folding.[14] The concept is shown in Fig. 3. It offers a number of advantages over the original shear design. Several obvious ones are that cutting a photonic-crystal is not required, the critical rows of half cylinders can be fabricated in separate locations, there is no need to shear the entire half crystal, possible vertical displacements are eliminated due to the folded membrane, the folded membrane acts as a superstrate (can be index matched to the substrate), and it is easier to integrate with the rest of the optical waveguide. Not shown in Fig. 3 is the lateral displacement actuator required to make the membrane translate, but this can be achieved using a voltage actuated interdigitated comb drive or a magnetic membrane translation scheme.[15]

In Fig. 4, we show that a photonic-crystal structure in which only half of the waveguide-row is translated functions
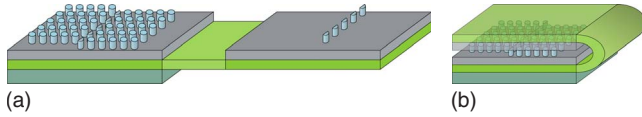
FIG. 3. (Color online) Membrane folding approach to fabricating a shear-tunable 2D photonic-crystal. (a) The bulk crystal consists of silicon (high index) rods on an SiO_2 (low index) thin film. Within the bulk crystal, one row consists of half cylinders or other shaped defects. On the adjoining membrane, the complementary row of half cylinders is fabricated. (b) Once folded over, the SiO_2 cladding is both above and below the 2D crystal for high confinement. Not shown are actuators that permit accurate lateral motion (indicated by the arrows) to tune the translation amount.

similarly to that of the original design (Fig. 2) in which half of the crystal is sheared. In addition, that half row may consist of ovals rather than half cylinders (as shown). Ovals are much simpler to fabricate than half cylinders. The main difference between the band diagrams of Fig. 2 and 4 is that in Fig. 4 the bands do not completely pull together at $s=0.5a$. In fact, if the structure in Fig. 4 is modified so that the upper half of the photonic-crystal bulk is offset by $0.5a$ and fixed in that location, then when the half row reaches $s=0.5a$ the bands do indeed pull together. However, there is no need to do this for the purpose of slowing down the group velocity of light.

If this device were fabricated, it might suffer from misalignment or accidental displacement of the sheared half row causing a gap between the two half rows which may arise from misalignment of the half row, variation in half-row feature sizes, or sidewall roughness. We analyzed this by simulating a gap of $0.2a$, shown in Fig. 5. (For an infrared photonic-crystal where a is approximately 500 nm; this corresponds to a 100 nm gap, which is a realistic upper limit on

the amount of gap error.) Now even at zero shear there exists a guided mode within the band gap; however, the device must now operate around $\omega=0.38\times2\pi c/a$ and can still be tuned from a group velocity of near zero (at the edge of the Brioullin zone with a shear of about $s=0.3a$) to near bulk at a shear of about $s=0.5a$. Therefore, although gap error significantly alters the band diagram, it does not significantly affect the tunable range of the device. Interestingly, we found that the gap effect can be further mitigated with an improved design. This is done by changing the shape of the half-row features as shown in Fig. 6, resulting in a device that can be tuned from a group velocity of near zero at $s=0.08a$ to near bulk at $s=0.5a$. It is worth noting that this particular implementation can realistically only be achieved using the membrane approach of Fig. 3, by placing one set of vertically oriented ovals on the folded membrane portion.

IV. TUNABLE COUPLED-RESONATOR OPTICAL WAVEGUIDE

A CROW consists of a periodic array of weakly coupled high-Q resonators, for example a periodic array of defects in a photonic-crystal, as shown in Fig. 1(c). If the resonators' quality factor Q is sufficiently high and the coupling between resonators is sufficiently weak, the photons are well confined inside the resonators. Therefore, photons can propagate only by evanescently coupling from one resonator to its nearest neighbor. In direct correspondence with the description of electrons in a strong periodic potential,[16] the guided modes of a CROW can be described using the tight binding approximation. A CROW is characterized by a nearly flat sinusoid dispersion relationship and can achieve group velocity smaller by several orders of magnitude than bulk material of the same average refractive index.[17–20] The guided modes of
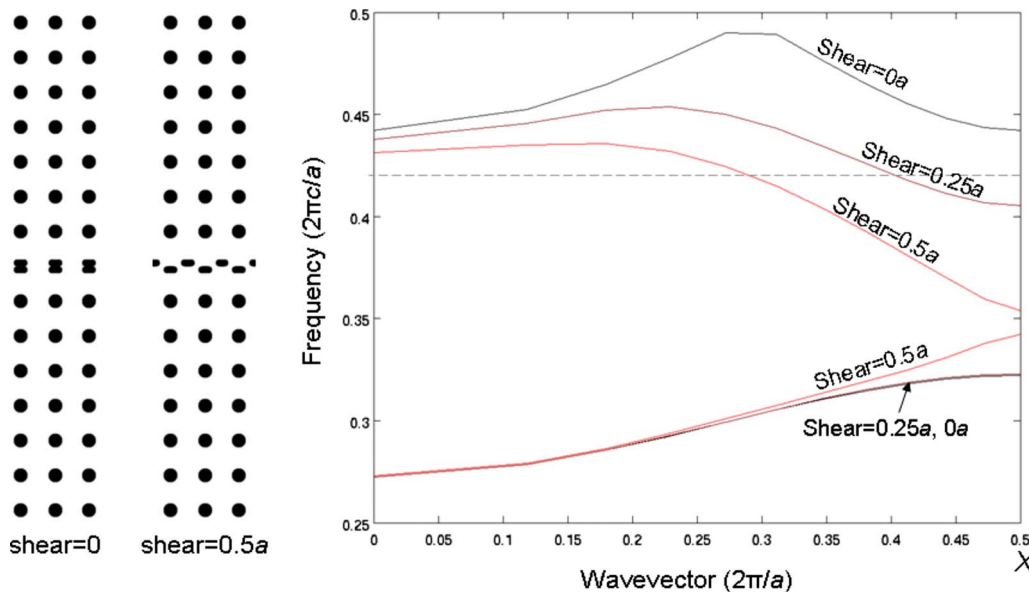

FIG. 4. (Color online) (Left) Illustration of the half-row translation scheme with oval-shaped features along the half rows, in the position of $s=0a$ and $s=0.5a$. (Right) Bandstructure of the two modes above and below the band gap for varying translation distance s of the upper half row. The dashed line indicates an example frequency ($0.42\times2\pi c/a$) at which the device might be used. At approximately $s=0.2a$ the group velocity of light is near zero; as s increases to $0.5a$ the group velocity approaches that of a bulk (averaged index) medium.
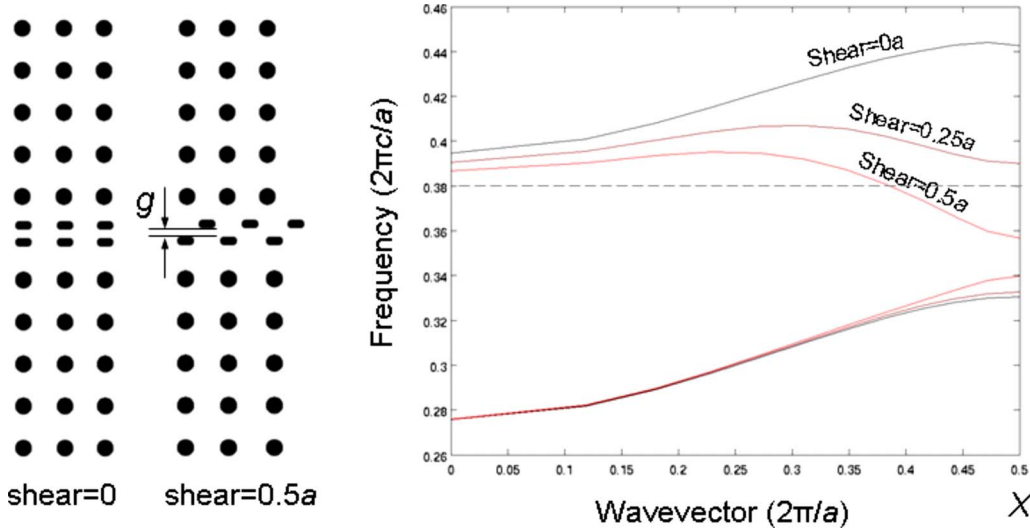
FIG. 5. (Color online) (Left) Illustration of how the gap error was simulated. (Right) Bandstructure of the modes around the band gap for varying shears. The dashed line indicates an example frequency at which the device might be used.

a CROW are well within the band gap and isolated from the continuum of modes that lie outside the band gap. This is in contrast with the previously shown design of Sec. II (and many other slow light waveguide designs)[21–26] which achieve low group velocity at the edge of Brillouin zone or band edge but at the cost of a large group velocity dispersion and poor confinement of the fields. The dispersion curve of CROW can be simply characterized by the coupling coefficient κ between nearest resonators, as done in Eq. (5) of Ref. 17. This equation states that the group velocity of a CROW is linearly proportional to the coupling coefficient κ, defined as the overlap of the eigenmodes of two adjacent resonators,

$$\kappa = \int d^3\mathbf{r}[\epsilon_0(\mathbf{r} - R\mathbf{e}_z) - \epsilon(\mathbf{r} - R\mathbf{e}_z)] \times \mathbf{E}_\Omega(\mathbf{r}) \cdot \mathbf{E}_\Omega(\mathbf{r} - R\mathbf{e}_z),$$

(1)

where $\mathbf{E}_\Omega(\mathbf{r})$ is the eigenmode with mode frequency Ω of individual resonators along a straight line parallel to the z axis and the coordinate of the center of the n-th resonator is $z = nR$. $\epsilon_0(\mathbf{r})$ is the dielectric constant of a single resonator while $\epsilon(\mathbf{r})$ is the dielectric constant of the entire CROW. Because the coupling coefficient depends on the exponential decay of evanescent waves between resonators in the coupling region, the imaginary part of the wave vector, $\Im\{\mathbf{k}\}$,
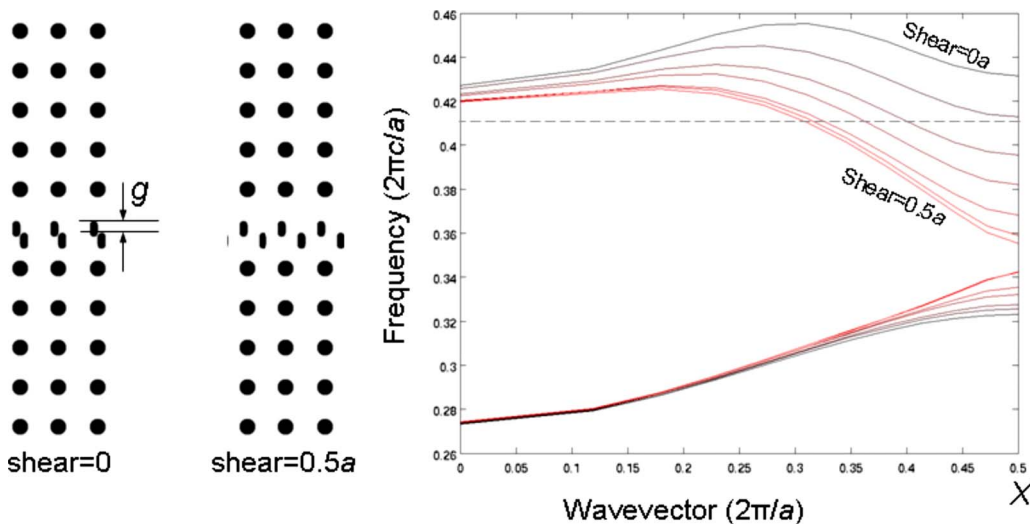

FIG. 6. (Color online) (Left) A modified tunable waveguide design using vertical dielectric ovals. One of the half rows is offset by a vertical gap $g = 0.2a$ and then translated laterally from $s = 0 - 0.5a$ for the simulation. (Right) Bandstructure of the two modes above and below the band gap for varying shears at a fixed gap. At the indicated operating frequency of $0.41 \times 2\pi c/a$, the group velocity can be tuned from slowest to fastest when s varies from $0.08a$ to $0.5a$.
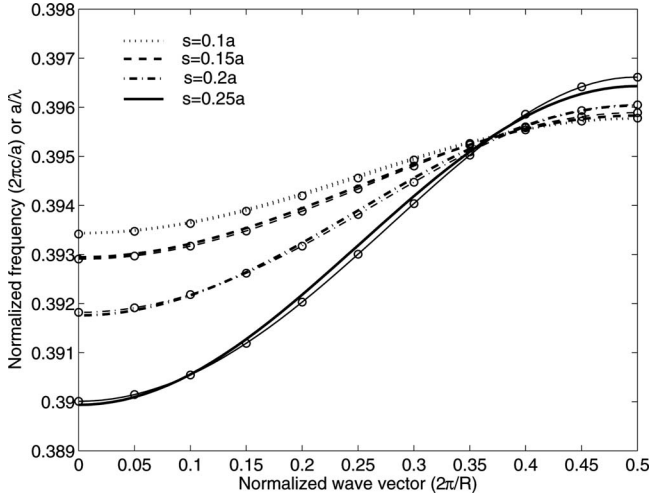
FIG. 7. The dispersion relation of the band within the band gap for a sheared CROW with different shear shifts s. Thin lines with circle symbols represent the spline fit with the exact simulation data, thick solid lines represent a least-squares cosinusoid fit. At $k = 0.5 \times \pi/R$ where the CROW systems have zero dispersion and maximum group velocity. CROWs operating at this point have far larger bandwidths than most other slow light devices.

plays an important role in this integral. The amplitude of $\mathbf{E}_\Omega(\mathbf{r})$ at $z = R$ [the center of $\mathbf{E}_\Omega(\mathbf{r} - R\mathbf{e}_z)$] decays as $\exp[-\Im\{\mathbf{k}\} \cdot (R-a)]$, where $R-a$ is the length of the coupling region. Therefore, κ is proportional to $\exp[-\Im\{\mathbf{k}\} \cdot (R-a)]$. In turn, the group velocity v_g is proportional to κ,[17] as we mentioned earlier. This implies that v_g in a CROW can be tuned in one of two possible methods. The first method is to adjust the intercavity distance R; the second method is to adjust the imaginary part of the wave vector $\mathbf{k}$. The imaginary part of $\mathbf{k}$ is proportional to the frequency difference between the edge of the frequency gap (i.e., band gap when $s=0$ or mode gap when $s \neq 0$)[12] and the mode frequency of individual resonators.[12,27] This difference in turn decreases as the shear shift increases from 0 to $a/2$, because of the shrinkage of the frequency gap as discussed in Sec. II and also seen in Fig. 7 of Reference. 7 Therefore, by actuation that specifies the shear between two half-infinite CROW lattices, we may alter the coupling efficiency between resonators and, hence, the group velocity.

We simulate the CROW structure of Figs. 1(c) and 1(d) at varying the shears using the parameters defined in the figure. In Fig. 7 we show the dispersion curve for the mode that appears within the band gap at varying amounts of shear. At
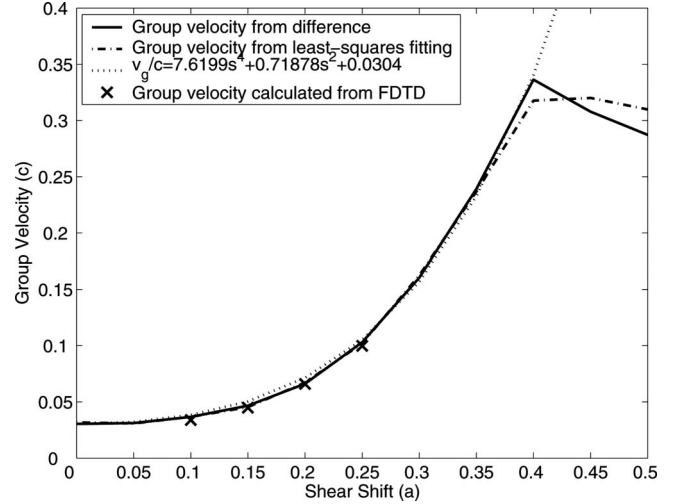

FIG. 8. Group velocity of the guided mode in sheared CROsWs versus the shear shift s.

$s = 0.25a$, the slope of the dispersion curve is larger indicating larger group velocity; at $s = 0.1a$, the group velocity is lower. We fit the data (circles in Fig. 7) to Eq. (5) of Ref. 17 using a least-squares cosinusoid fit as thick solid lines in Fig. 7, to estimate the coupling coefficient κ. These data, along with calculations of group velocity at $k = 0.5 \times \pi/R$ for each shear shift are listed in Table I.

In order to obtain an approximate analytical dependence of the group velocity on the shear shift, we calculated band diagrams for more shear shifts than these shown in Table I. The results, for shear shift ranging from zero to half the lattice constant, are shown in Fig. 8. Polynomial fitting of the data in Fig. 8 revealed that the dependence of v_g on s is quartic, given by $v_g = (7.6199s^4 + 0.7188s^2 + 0.0304)c$.

The group velocity can be tuned from $0.0304c$ with $s = 0$ to $0.336c$ with $s = 0.4a$. The discrepancy at shear shift larger than $0.4a$ is because of the failure of evanescent coupling in the coupling region. When the shear shift is larger than $0.4a$, the mode gap becomes too small (Fig. 7 of Ref. 7) to accommodate the guide modes of CROW,[30] so the guided modes of CROW is coupled with the guided modes of sheared photonic-crystal. In this regime, the resonators are coupled by propagating rather than evanescent waves, invalidating the tight binding approximation. This situation looks more like a photonic-crystal waveguide than a CROW. This is verified in Fig. 9, which depicts the y component of the

TABLE I. Coupling coefficients and group velocities for sheared CROWs with different shear shifts. The dispersion curves are shown in Fig. 7.

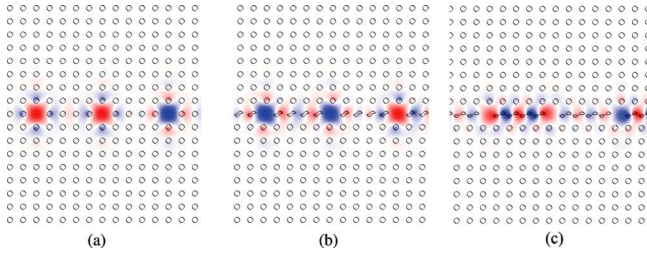| Shear shift s	Coupling coefficient κ	Group velocity (Least-squares fit)	Group velocity (Direct difference)	Group velocity (FDTD)
$0.1a$	3.0×10^{-3}	$0.0367c$	$0.0367c$	$0.0338c$
$0.15a$	3.7×10^{-3}	$0.0466c$	$0.0454c$	$0.0448c$
$0.2a$	5.4×10^{-3}	$0.0661c$	$0.0672c$	$0.0659c$
$0.25a$	8.3×10^{-3}	$0.102c$	$0.103c$	$0.0998c$

FIG. 9. (Color online) The electric field y component (out-of-the-page) for the guided mode of the CROW (a) with $s=0$ at $k=0.5\times\pi/R$, (b) with $s=0.25a$ at $k=0.5\times\pi/R$, (c) $s=0.5a$ at $k=0.5\times\pi/R$.

electric field corresponding to the eigenstate of the sheared CROW for $s=0$, 0.25, and 0.5a at $k=0.5\times\pi/R$. The onset of lack of light confinement becomes clear by comparing the modes at each shear position. The fraction of electric field energy in the resonators in Fig. 9 is 59.5%, 50.5% and 28.2%, respectively. At the lower shear values, even though the resonators are of low refractive index they confine light strongly. This is why in Fig. 7 the smaller shear shift simulations have better least-squares fits; the tight binding approximation holds better. It is worth noting that the mirror symmetry about the z axis in the case of $s=0$ is broken when $s=0.25a$ or 0.5a. At zero shear shift, the eigenstate is four-fold symmetric and has four symmetry axes (mirror planes) $\mathbf{e}_z$, $\mathbf{e}_x$, $1/\sqrt{2}(\mathbf{e}_x+\mathbf{e}_z)$, and $1/\sqrt{2}(\mathbf{e}_x-\mathbf{e}_z)$ while at $s=0.25a$ or 0.5a it is only two-fold symmetric and has no mirror symmetry, as expected.

We also simulated light propagation in sheared CROWs using FDTD to verify the preceding analysis. The first cavity was excited with a Gaussian pulse of time $T_0=750a/c$, chosen such that the pulse bandwidth would be 1/4 of the CROW guided mode bandwidth for $s=0.1a$. This shear value corresponds to the slowest structure studied and we chose it to avoid dispersion contaminating our analysis of group velocity. We simulated structures having shears of $s=0.1a$, s

$=0.15a$, $s=0.2a$, and $s=0.25a$. From the fixed time snapshot of each simulation at $t=3850a/c$, it is obvious that the pulse in a sheared CROW having $s=0.1a$ [Fig. 10(d)] propagates slowest, while the pulse in a sheared CROW having $s=0.25a$ [Fig. 10(a)] propagates fastest. The spatial duration of the pulses in the sheared CROW are $L_0=T_0 v_g$, meaning that the length of each pulse is proportional to its group velocity. Figure 10 also shows that the shortest (slowest) pulse occurs with $s=0.1a$, and longest (fastest) pulse occurs with $s=0.25a$.

We also analyzed group velocity by measuring the time it took the pulse peak to propagate from plane A to plane B in the CROW of Fig. 10 for different amounts of shear shift $s=0.1a$, 0.15a, 0.2a, and 0.25a. This method of determining v_g is acceptable because dispersion is negligible for the chosen T_0. The group velocities calculated from FDTD are listed in Table I and labeled as "x" in Fig. 8. Thus, the FDTD simulations demonstrate good agreement with the predictions from band diagrams and the polynomial fit of v_g vs s.

V. TUNABLE CROW WITH SIDE-CAVITIES

The simulated group velocity tuning range in Sec. IV, from 0.0304c to 0.336c, is not the limit of our tunable CROWs. In principle, we can achieve a tunable range down to arbitrarily small group velocities by increasing the intercavity distance. Beyond a limited extent this becomes impractical because it requires enlarging the lateral dimensions of the device; in addition, dispersion becomes non-negligible as the intercavity distance increases. A better way is to place one or more side cavities in the neighborhood of each individual resonator in the CROW, as shown in Fig. 11 and first proposed in Ref. 8. In previous work on similar structures, the group velocity was reduced by modulating the refractive index of a small rod within the side cavities[8,9] and the cavities along the CROW.[8] This shifts the resonance of each cavity and allows one to tune the structure such that the light
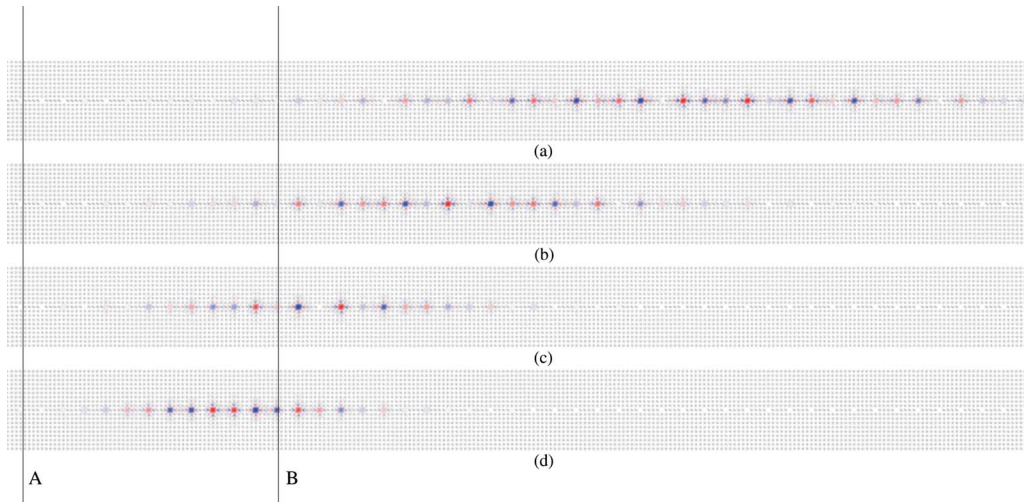

FIG. 10. (Color online) Snapshots of the electric field in tunable CROWs at $t=3850a/c$. Gaussian pulses propagate inside tunable CROWs (a) with $s=0.25a$, (b) with $s=0.2a$, (c) with $s=0.15a$, and (d) with $s=0.1a$. The duration time of the pulses is 750a/c. As we have observed earlier, the electric field is primarily concentrated within the resonators for these shear amounts; dispersion is negligible.
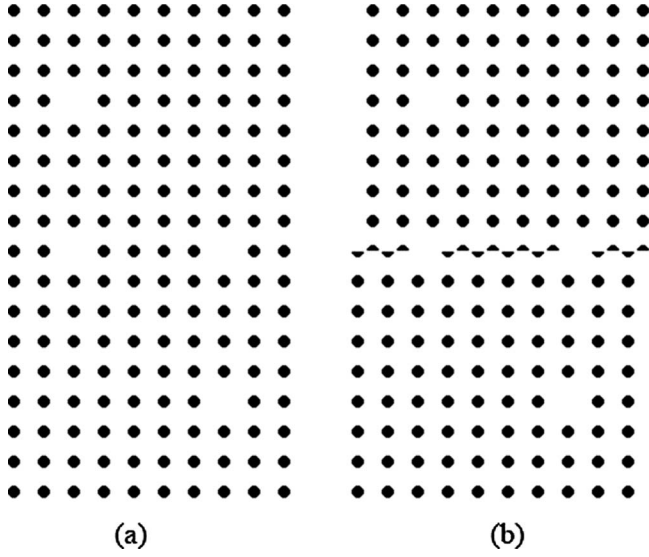
FIG. 11. (a) A supercell of the photonic-crystal CROW with side cavities at the half shear position. (b) At the zero shear position. For these simulations, the entire half of the crystal is sheared as shown (instead of a half-defect row).

is in resonance with the side cavities and is trapped there, effectively in a flat band state.

Here, we aim to achieve a larger group velocity tuning range until a similar flat band state by shearing a CROW with side cavities. Instead of changing the resonance frequencies of the cavities, we are effectively changing the coupling between adjacent resonators in the CROW as well the coupling between side cavities and the CROW by shearing. The transmission matrix for a CROW section as the function of its length l is

$$T(l) = \begin{pmatrix} e^{-j\beta l} & 0 \\ 0 & e^{-j\beta l} \end{pmatrix}, \qquad (2)$$

where β is the Bloch wave vector of the CROW. It has a sinusoidal relationship to the frequency ω as

$$\omega = \omega_C[1 - \kappa \cos(\beta R)], \qquad (3)$$

where ω_C is the center frequency and κ is the coupling coefficient between adjacent resonators. They are both functions of the shear shift, and can be obtained from the data in Sec. IV.

We assume that the side cavities have resonant frequency ω_A, that does not change during shearing. The side cavities couple to the CROW with time constant τ, which is also the function of the shear shift. The direct coupling between the side cavities can be ignored. Therefore, the transmission matrix for the side coupling of the CROW to a side cavity can be expressed as

$$T_A = \begin{pmatrix} 1 + \dfrac{j}{(\omega - \omega_A)\tau} & \dfrac{j}{(\omega - \omega_A)\tau} \\ -\dfrac{j}{(\omega - \omega_A)\tau} & 1 - \dfrac{j}{(\omega - \omega_A)\tau} \end{pmatrix}. \qquad (4)$$

The transmission matrix through an entire period can then be determined as

$$T(l) = T_A T(R - s) T_A T(R + s), \qquad (5)$$

where s is the shear shift. The Bloch-Floquet condition is $\det(T - \mu I) = 0$. Since $\det(T) = 1$, $\mu = \exp(\pm jk2R)$ if μ reduces to a pure phase shift (e.g., for guided modes), where $2R$ is the length of one period and k corresponds to the Bloch wave vector of the entire system. Since μ can be calculated as $\mu = \frac{1}{2}(\mathrm{Tr}(T) \pm j\sqrt{4 - \mathrm{Tr}^2(T)})$, the band diagram of the system can be obtained as

$$\cos(2kR) = \frac{1}{2}\mathrm{Tr}(T) = \cos(2\beta R) + \frac{\cos(2\beta s) - \cos(2\beta R)}{(\omega - \omega_A)^2 \tau^2}$$
$$+ \frac{2\sin(2\beta R)}{(\omega - \omega_A)\tau}. \qquad (6)$$

Guided modes exist in the frequency range where $\left|\frac{1}{2}\mathrm{Tr}(T)\right| \le 1$, while the system has mode gaps in the frequency range of $\left|\frac{1}{2}\mathrm{Tr}(T)\right| > 1$. The typical band diagram for sheared CROW with side cavities is shown in Fig. 12(a). There are four guided modes and a gap in the vicinity of the resonance of side cavities. This mode structure arises from the coupling between guided modes from the sheared CROW and the resonant modes of the side cavities. As the shear decreases, the coupling coefficient κ between adjacent resonators in the CROW decreases while the coupling coefficient $1/\tau$ between side cavities and the CROW increases. The decrease in the coupling coefficient between adjacent resonators in the CROW is equivalent to pulling point A in Fig. 12 downward while the increase in the coupling coefficient between side cavities and the CROW is equivalent to pushing point B upward. Therefore, the group velocity is tuned to a slower value.

By directly solving Maxwell equations in the Fourier domain,[10] we obtained the photonic bands from the structure in Fig. 11 for different shear shifts, shown in Fig. 12(b). It proves our prediction from transmission matrix analysis. The group velocity can be tuned as low as $\sim 10^{-3}c$.

In order to achieve even lower group velocity until flat band, we can utilize different resonant frequencies for side cavities, e.g., design the side cavities of the lower and upper half to have different resonant frequencies, ω_A and ω_B, respectively. This can be achieved by leaving some material inside the side cavities and/or tuning the refractive index of left material. The transmission matrix through an entire period need then be modified as

$$T(l) = T_A T(R - s) T_B T(R + s), \qquad (7)$$

where T_B is given by the same formula as T_A (Eq. (4)), except replacing ω_A with ω_B. The band diagram can then be obtained similarly as

$$\cos(2kR) = \frac{1}{2}\mathrm{Tr}(T) = \cos(2\beta R) + \frac{C_+}{\omega - \omega_A} + \frac{C_-}{\omega - \omega_B}, \qquad (8)$$
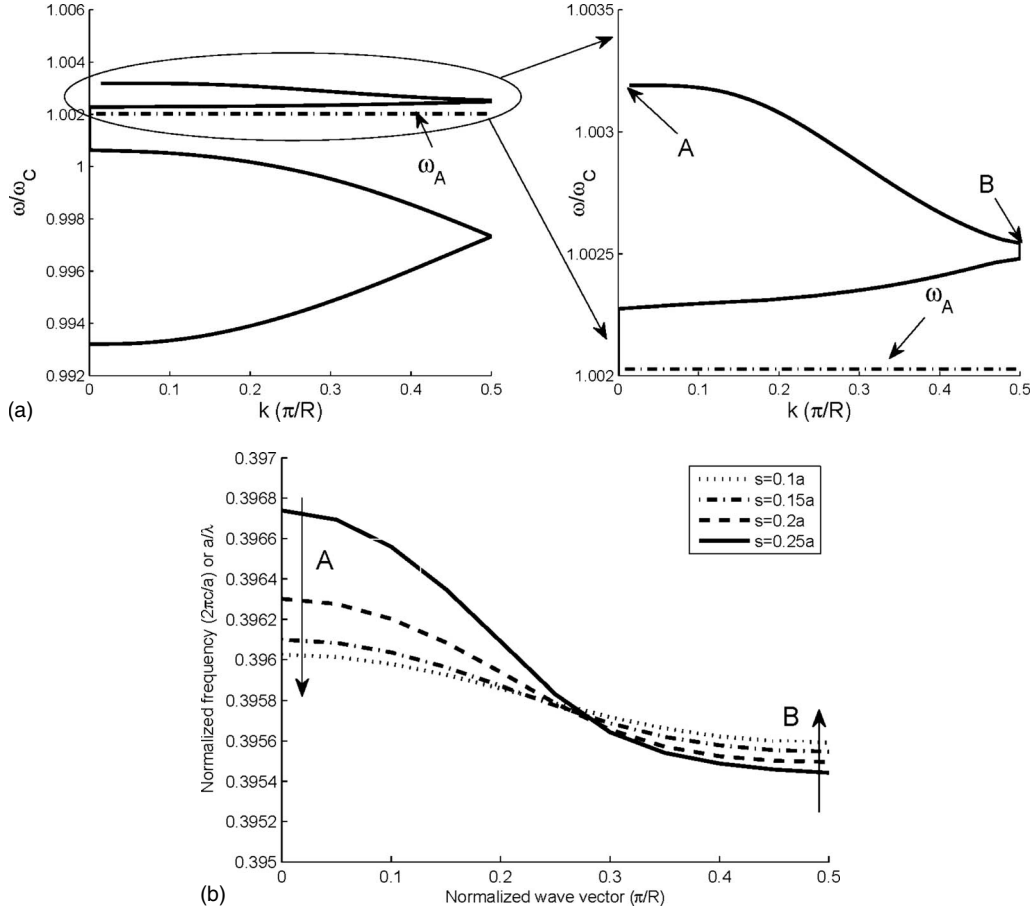
where

FIG. 12. (a) Band diagram of sheared CROW with side cavities (Fig. 11) from transmission matrix calculation for $s=0.1a$. The center frequency and coupling coefficient between adjacent resonators of the CROW can be obtained from the data of Sec. IV as $\omega_C =0.3946(2\pi c/a)$ and $\kappa=0.003$. The side cavity resonance frequency is $\omega_A=0.3954(2\pi c/a)$, and the coupling rate is $1/\tau=\omega_A/1200$. (b) Band diagram of sheared CROW with side cavities (Fig. 11) for $s=0.1a\sim0.25a$. As the shear decreases, the guided mode becomes flatter.

$$C_{\pm} = \pm \frac{\cos(2\beta s) - \cos(2\beta R)}{(\omega_A - \omega_B)\tau^2} + \frac{\sin(2\beta R)}{\tau}. \qquad (9)$$

As shown in Fig. 13(a), the band diagram still has four guided modes in the vicinity of the resonances, but now with two gaps occurring around ω_A and ω_B. From Eqs. (8) and (9), the guided mode between ω_A and ω_B depends strongly on the dispersion relationship $\beta(\omega)$ of the original CROW without side cavities. It is also illustrated in Fig. 13(b) where $\beta(\omega)$ is tuned by changing the coupling coefficient κ between adjacent resonators in the CROW (following Eq. (3)) through shearing. In this case, the group velocity can easily be tuned lower than in the case of $\omega_A=\omega_B$, e.g., at least one order of magnitude lower in Fig. 13. Therefore, we can achieve a tunable range of group velocity spanning at least three orders of magnitude ($\sim10^{-4}c$ to $\sim10^{-1}c$).

With deliberate design of ω_A and ω_B, the shearing can result in the group velocity tuning to even lower values until the flat band emerges at $\omega=\omega_A$ when

$$C_+(\omega_A) = \frac{\cos[2\beta(\omega_A)s] - \cos[2\beta(\omega_A)R]}{(\omega_A - \omega_B)\tau^2} + \frac{\sin[2\beta(\omega_A)R]}{\tau}$$

$$= 0; \text{ and} \qquad (10)$$

$$\left| \frac{1}{2}\text{Tr}(T) \right| = \left| \cos[2\beta(\omega_A)R] + \left. \frac{dC_+}{d\omega} \right|_{\omega=\omega_A} + \frac{C_-(\omega_A)}{\omega_A - \omega_B} \right|$$

$$= \left| \left(1 + \frac{2R}{v_g(\omega_A)\tau} \right)\cos[2\beta(\omega_A)R] \right.$$

$$+ \frac{2}{(\omega_A - \omega_B)\tau}\left(1 + \frac{R}{v_g(\omega_A)\tau} \right)\sin[2\beta(\omega_A)R]$$

$$\left. - \frac{2s}{(\omega_A - \omega_B)v_g(\omega_A)\tau^2}\sin[2\beta(\omega_A)s] \right| \le 1,$$

$$(11)$$

where $v_g=\frac{d\omega}{d\beta}$ is the group velocity of the original sheared CROW without side cavities. It can be calculated as $v_g =\omega_C\kappa R \sin(\beta R)$ for our case. To achieve flat band at zero shift, Eqs. (10) and (11) can be further simplified as

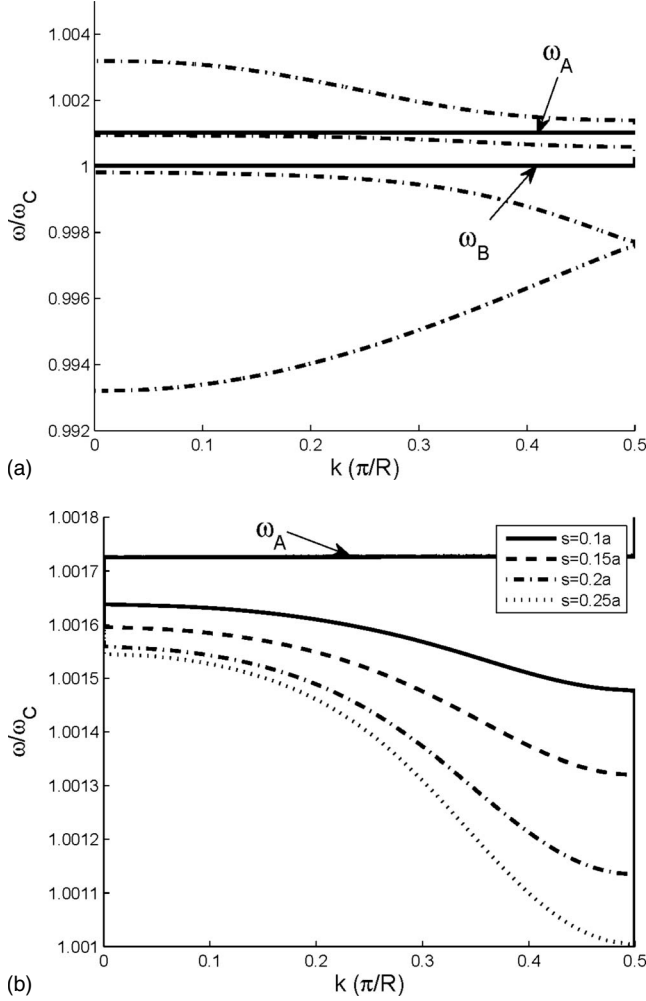$$\tan[\beta(\omega_A)R]=-(\omega_A - \omega_B)\tau, \qquad (12)$$

FIG. 13. Band diagram of sheared CROW with side cavities (Fig. 11) of different resonant frequencies $\omega_A \neq \omega_B$ from transmission matrix calculation. (a) $s=0.2a$. The center frequency and coupling coefficient between adjacent resonators can be obtained from the data of Section IV as $\omega_C=0.3939(2\pi c/a)$ and $\kappa=0.0054$. The side cavity resonance frequencies are $\omega_A=0.3953(2\pi c/a)$ and $\omega_B=0.3946(2\pi c/a)$, respectively. The coupling rate is $1/\tau=\omega_A/1400$. (b) $s=0.1a \sim 0.25a$.

$$\left| \left(1 + \frac{2R}{v_g(\omega_A)\tau}\right) + 2\,\cos^2[\beta(\omega_A)R] \right| \leq 1. \qquad (13)$$

From Eqs. (12) and (13), we can see that the original CROW needs to have negative group velocity to satisfy the flat band conditions for zero shift. Note that the requirement of negative group velocity is not necessary for flat bands at other shear shifts. Negative group velocity is very common and easy to achieve for CROW systems with deliberate design, e.g., by tuning the intercavity distance.[17]

It is worth noting that similar flat band conditions can also be obtained from Eq. (6) when the side cavities of lower and upper half have the same resonant frequency.

$$\sin[2\beta(\omega)R] = O(\omega - \omega_A), \qquad (14)$$

$$\cos[2\beta(\omega)s] - \cos(2\beta R) = O((\omega - \omega_A)^2), \qquad (15)$$

$$\left| \cos[2\beta(\omega_A)R] + \left. \frac{\mathrm{d}^2\left(\dfrac{\cos(2\beta s) - \cos(2\beta R)}{\tau^2}\right)}{\mathrm{d}\omega^2} \right|_{\omega=\omega_A} \right.$$
$$\left. + \left. \frac{\mathrm{d}\left(\dfrac{2\,\sin(2\beta R)}{\tau}\right)}{\mathrm{d}\omega} \right|_{\omega=\omega_A} \right|$$
$$= \left| \left(1 + \frac{2R}{v_g(\omega_A)\tau}\right)^2 \cos[2\beta(\omega_A)R] \right.$$
$$+ \frac{2RD(\omega_A)}{\tau^2}\sin[2\beta(\omega_A)R] - \frac{4s^2}{v_g^2(\omega_A)\tau^2}\cos[2\beta(\omega_A)s]$$
$$\left. - \frac{2sD(\omega_A)}{\tau^2}\sin[2\beta(\omega_A)s] \right| \leq 1, \qquad (16)$$

where $D=\frac{\mathrm{d}^2\beta}{\mathrm{d}\omega^2}$ is the dispersion parameter of the original sheared CROW without side cavities.

If the side cavities of the lower and upper half have different resonant frequencies and conditions (10) and (11) are satisfied, then flat band can be achieved at any value of shear shift. But from Eqs. (14)–(16), we can see that when the side cavities of the lower and upper half have the same resonant frequency, flat band can only be achieved at $s=0$, and the following conditions have to be satisfied.

$$\sin[2\beta(\omega_A)R] = 0, \qquad (17)$$

$$\left| 1 + \frac{2R}{v_g(\omega_A)\tau} \right| \leq 1. \qquad (18)$$

The same as $\omega_A \neq \omega_B$, it also requires that the original CROW has negative group velocity, that is true for the example in the Ref. 8 although it is not discussed.

Therefore, the structure as presented is dynamically tunable, and by adiabatically shearing should be able to coherently slow down, hold, and speed up an optical signal in the same fashion as shown in Refs. 8 and 9 but by only modifying structure configuration.

VI. CONCLUSION

We have designed a slow light device with a mechanically tunable waveguide region to realize active control of the group velocity of light. The tuning range is over three orders of magnitude with low dispersion by means of a flat band side cavity configuration and may even exceed this amount with improvements to the basic design. This potentially allows one to reversibly slow down, store, and release a pulse of light without significant dispersion by simply shearing the crystal, as long as the shearing is done adiabatically. This capability and the ability to tune the group velocity hold promise for optical communications as well as classical and quantum optical information processing.

*ktian@us.ibm.com

[1] L. V. Hau, S. E. Harris, Z. Dutton, and C. H. Behroozi, Nature (London) **397**, 594 (1999).

[2] M. D. Stenner, D. J. Gauthies, and M. A. Neifeld, Nature (London) **425**, 695 (2003).

[3] M. S. Bigelow, N. N. Lepeshkin, and R. W. Boyd, Science **301**, 200 (2003).

[4] K. Lee and N. M. Lawandy, Appl. Phys. Lett. **78**, 703 (2001).

[5] Y. Okawachi, M. S. Bigelow, J. E. Sharping, Z. Zhu, A. Schweinsberg, D. J. Gauthier, R. W. Boyd, and A. L. Gaeta, Phys. Rev. Lett. **94**, 153902 (2005).

[6] Y. A. Vlasov, M. O'Boyle, H. F. Hamann, and S. J. McNab, Nature (London) **438**, 65 (2005).

[7] K. Tian, G. Barbastathis, and J. Hong, Opt. Express **14**, 10887 (2006).

[8] M. F. Yanik and S. Fan, Phys. Rev. Lett. **92**, 083901 (2004).

[9] M. F. Yanik, W. Suh, Z. Wang, and S. Fan, Phys. Rev. Lett. **93**, 233903 (2004).

[10] S. G. Johnson and J. D. Joannopoulos, Opt. Express **8**, 173 (2001).

[11] H. A. Haus, *Waves and Fields in Optoelectronics* (Prentice-Hall Englewood Cliffs, New Jersey, 1984).

[12] A. Mekis, S. Fan, and J. D. Joannopoulos, Phys. Rev. B **58**, 4809 (1998).

[13] W. J. Arora, S. Sijbrandij, L. Stern, J. Notte, H. I. Smith, and G. Barbastathis, J. Vac. Sci. Technol. B **25**, 2184 (2007).

[14] A. J. Nichol, P. S. Stellman, W. J. Arora, and G. Barbastathis, Microelectron. Eng. **84**, 1168 (2007).

[15] A. J. Nichol, W. J. Arora, and G. Barbastathis, 2007 IEEE/LEOS International Conference on Optical MEMS and Nanophotonics 2007 (unpublished) p. 189.

[16] N. W. Ashcroft and N. D. Mermin, *Solid State Physics* (Harcourt Brace Jovanovich, Orlando, 1976).

[17] A. Yariv, Y. Xu, R. K. Lee, and A. Scherer, Opt. Lett. **24**, 711 (1999).

[18] Y. Xu, R. K. Lee, and A. Yariv, J. Opt. Soc. Am. B **17**, 387 (2000).

[19] H. Altug and J. Vuckovic, Appl. Phys. Lett. **84**, 161 (2004).

[20] H. Altug and J. Vuckovic, Appl. Phys. Lett. **86**, 111102 (2005).

[21] R. D. Meade, A. Devenyi, J. D. Joannopoulos, O. L. Alerhand, D. A. Smith, and K. Kash, J. Appl. Phys. **75**, 4753 (1994).

[22] A. Mekis, J. C. Chen, I. Kurland, S. Fan, P. R. Villeneuve, and J. D. Joannopoulos, Phys. Rev. Lett. **77**, 3787 (1996).

[23] S. G. Johnson, S. Fan, P. R. Villeneuve, J. D. Joannopoulos, and L. A. Kolodziejski, Phys. Rev. B **60**, 5751 (1999).

[24] S. G. Johnson, P. R. Villeneuve, S. Fan, and J. D. Joannopoulos, Phys. Rev. B **62**, 8212 (2000).

[25] S. Y. Lin, E. Chow, V. Hietala, P. R. Villeneuve, and J. D. Joannopoulos, Science **282**, 274 (1998).

[26] M. Notomi, K. Yamada, A. Shinya, J. Takahashi, C. Takahashi, and I. Yokohama, Phys. Rev. Lett. **87**, 253902 (2001).

[27] P. Yeh, *Optical Waves in Layered Media* (Wiley, New York, 1988).

[28] A. Konig and N. D. Mermin, Phys. Rev. B **56**, 13607 (1997).

[29] Based on group theory, sheared photonic-crystal has a nonsymmorphic space group which can provide this additional degeneracy at $k = 0.5(2\pi/a)$.[28]

[30] Although the mode gap for $s > 0.4a$ is too mall for the guided modes of CROW, they are still well inside the band gap of perfect photonic-crystals. Therefore, the modes of individual resonators delocalize only along the shear plane, but not vertically in the entire photonic-crystal because the modes are confined along the shear plane by the mode gap while confined in other directions by the band gap.